Supplementary files

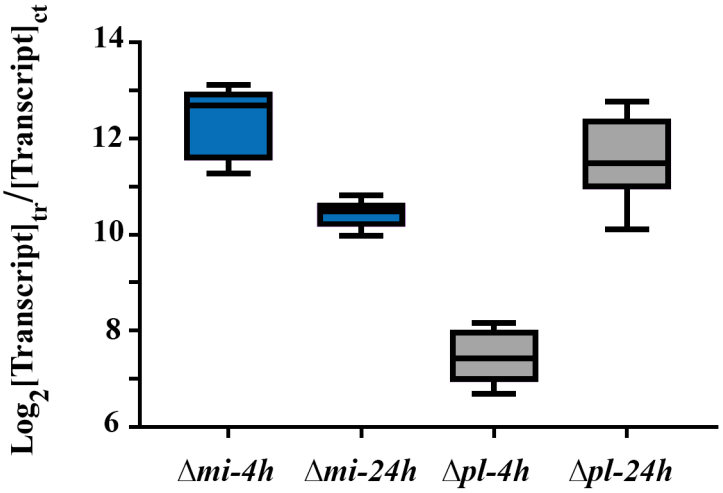

Supplementary Fig. 1. Temporal fingerprinting of miR4673. The expression level of miR4673 as detected by stem-loop qPCR in samples treated with naked miRNA (Δmi) and the plasmid encoding miR4673 (Δpl) compared to control cells (tr: transfected; ct: control; n=3 biological samples/time point).

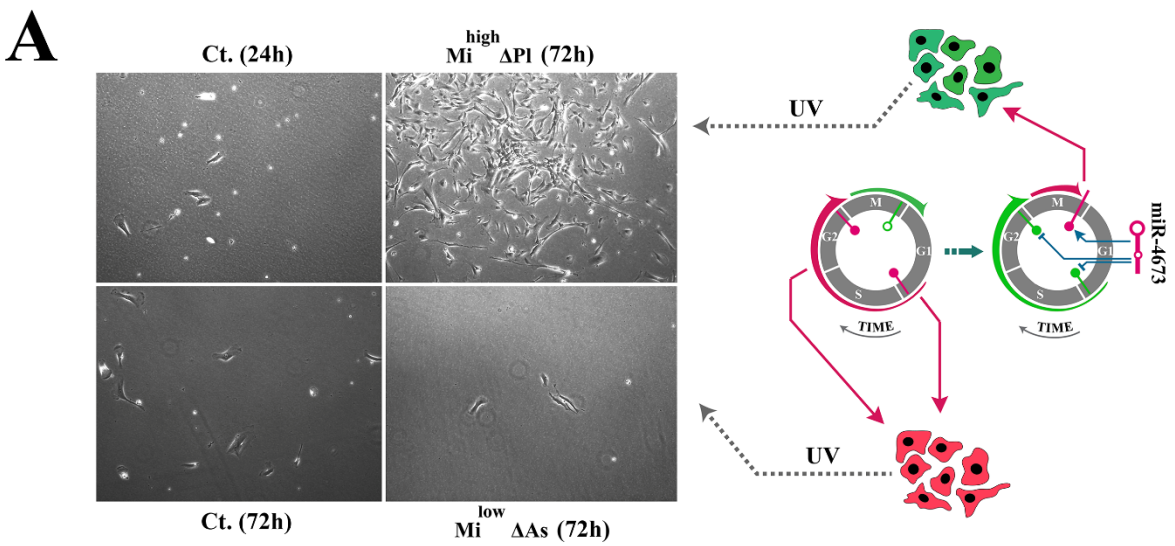

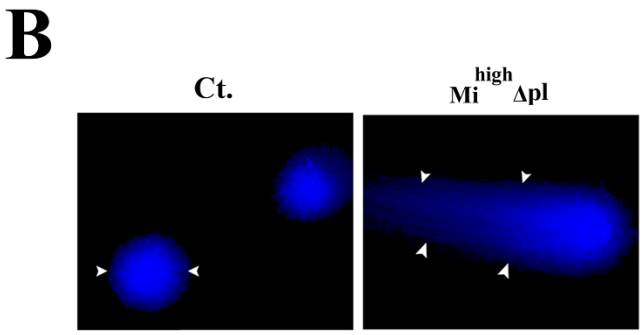

Supplementary Fig. 2. Functional assessment of cell cycle checkpoint modulation by miR4673 signalling. (A) After exposure to UVC (see methods) mi^{high}Δpl neural progenitors evaded apoptosis due to suppressed p53/p21/p27 cascades. Few surviving control cells remained quiescent post-exposure. Lowest survival rate post-exposure was observed in mi^{low}ΔAs cells due to hyperactivity of G1-S checkpoint machinery. (B) Neutral comet assay confirmed enhanced accumulation of DNA double stranded breaks in mi^{high}Δpl neural progenitors due to suppressed p53/p21 and silenced G1 checkpoint machinery. It is important to note that the accumulation of double-stranded breaks in in mi^{high}Δpl neural progenitors reflects constant expression of miR4673 at a high supra-physiological level (see Supplementary Fig. 1). The endogenous expression level of miR4673 is several orders of magnitude lower than the plasmid-driven expression level.

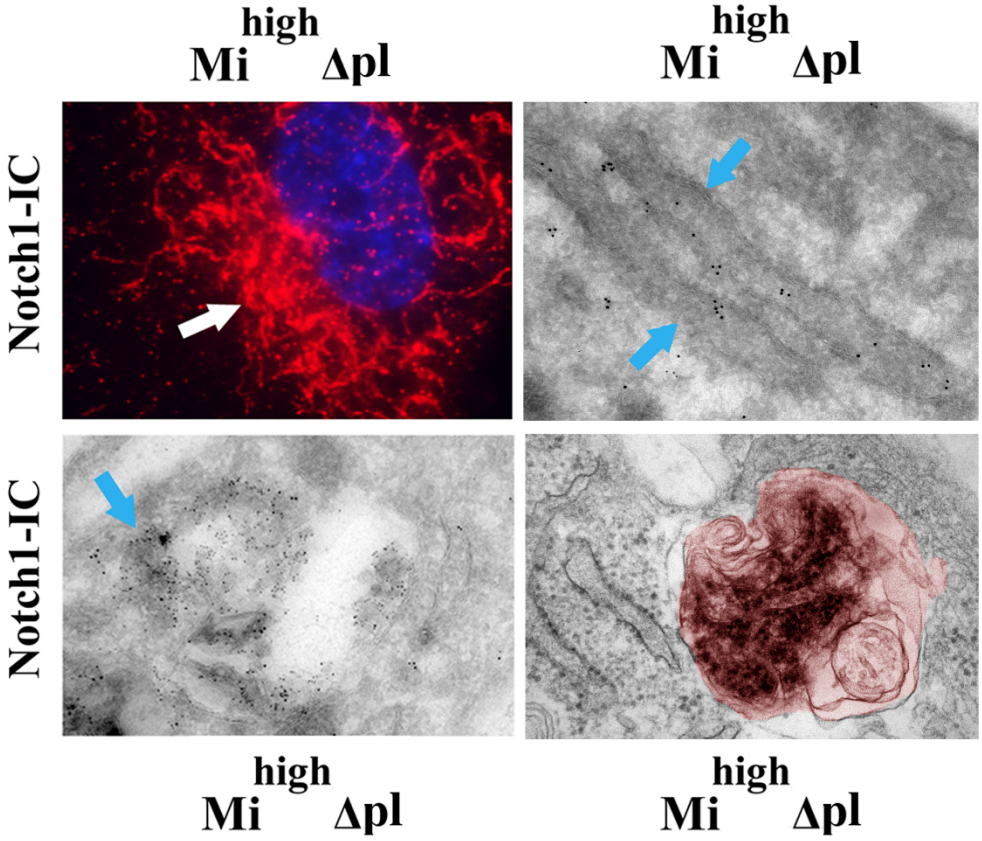

Supplementary Fig. 3. Autophagic depletion of activated Notch-1. Notch-1^{IC} (cleaved intracellular Notch-1) was localized to an expanded endoplasmic reticulum in mi^{high}Δpl cells (top left) confirmed also by immuno-gold labelling (top right, blue arrows demonstrate the endoplasmic reticulum). Immuno-gold labelling showed final degradation of activated Notch-1^{IC} in autophagosomes of mi^{high}Δpl cells (bottom, blue arrow shows the outer membrane of an autophagosome that has engulfed Notch-1^{IC})

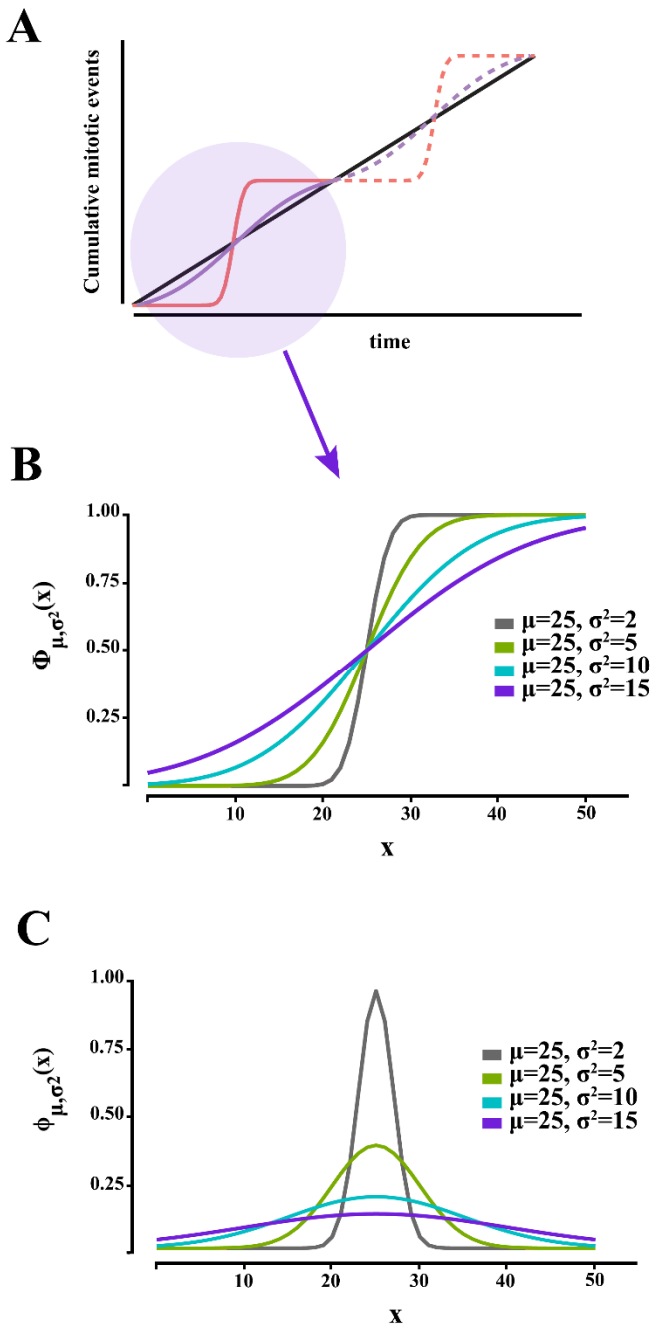

Supplementary Fig. 4. Mathematical interpretation of the cumulative mitotic landscape. Each mitotic wave in the graph (purple circle in A) represents the cumulative normal distribution of mitotic events (B) in a defined period of time. Deviations from linearity in B correspond to the standard deviation of the normal distribution curve (C). Synchronicity of mitotic events leads to a smaller standard deviation in the normal distribution curve and a steeper transition in the cumulative graph (compare the grey and the purple curves in B and C).

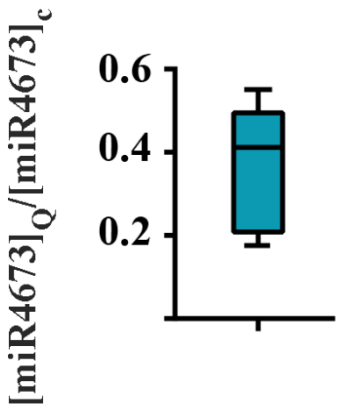

Supplementary Fig. 5. Expression of miR4673 in quiescent (Q) cells normalized to the cycling progenitor cells (c).

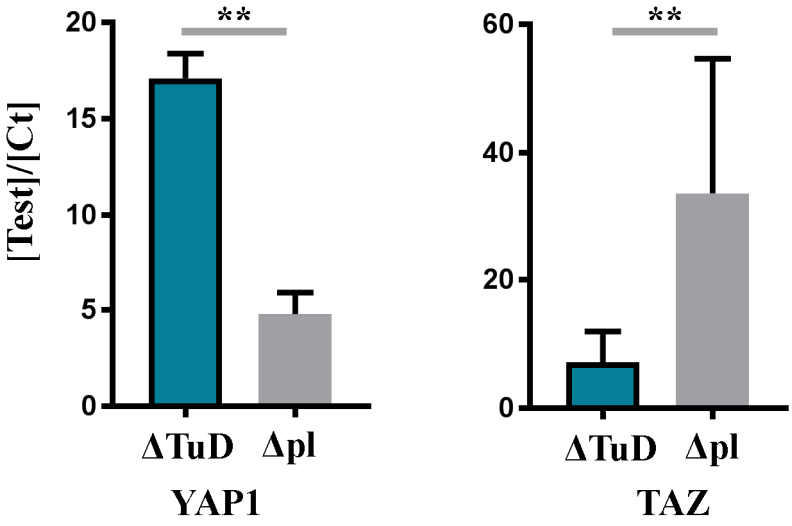

Supplementary Fig. 6. Transcriptional profile of Yap1 and Taz subsequent to the amplification (Δpl) and inhibition (ΔTuD) of miR4673 in the growth medium. All values are normalised to β-actin.

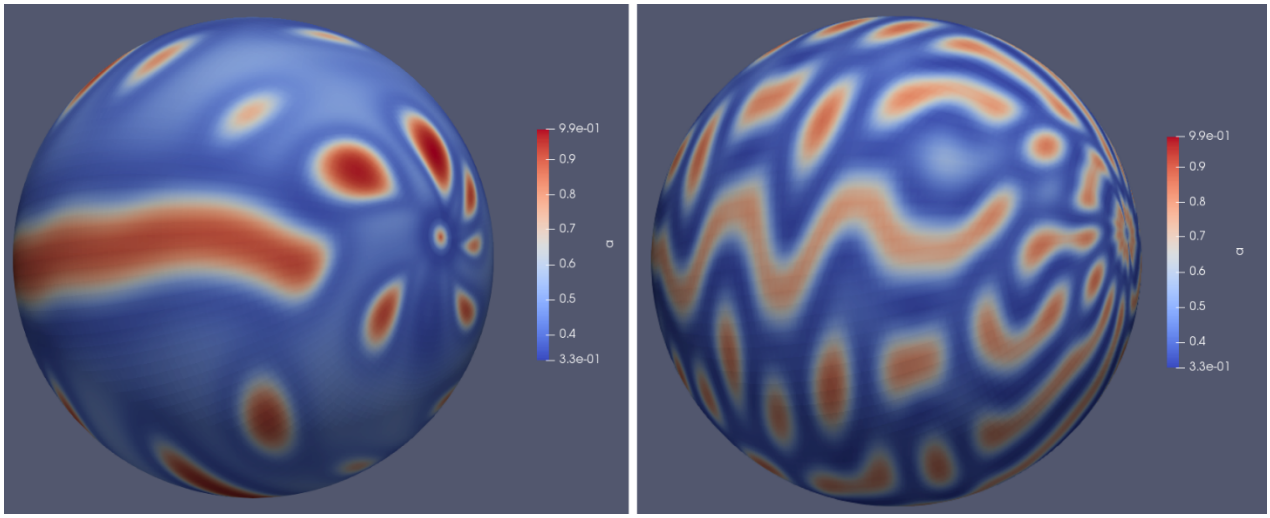

Supplementary Fig. 7. Mathematical modelling of brain morphogenesis based on reaction-diffusion model. The topographical maps were generated using READY and based on the parameters that integrate findings from the bimodal regulation of cell cycle into the reaction-diffusion equations (left: macaque brain; right: human brain). Concentration of morphogens U is shown on a scale from 0 to 1 (supplementary methods).

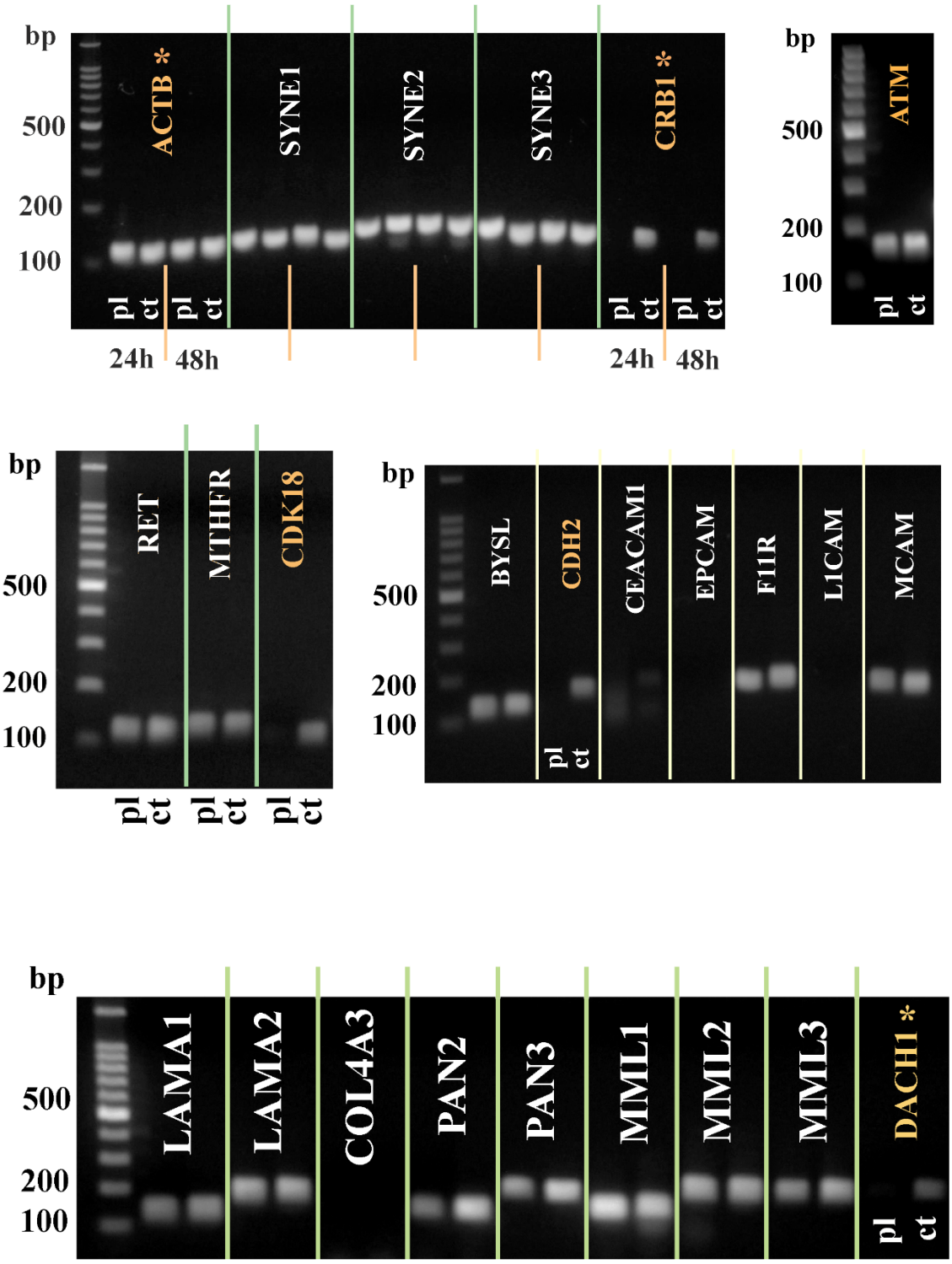
bp
500
200
100
ACTB *
SYNE1
SYNE2
SYNE3
CRB1 *
pl
ct
24h
48h
ATM
RET
MTHFR
CDK18
BYSL
CDH2
CEACAM1
EPCAM
F11R
L1CAM
MCAM
LAMA1
LAMA2
COL4A3
PAN2
PAN3
MML1
MML2
MML3
DACH1 *

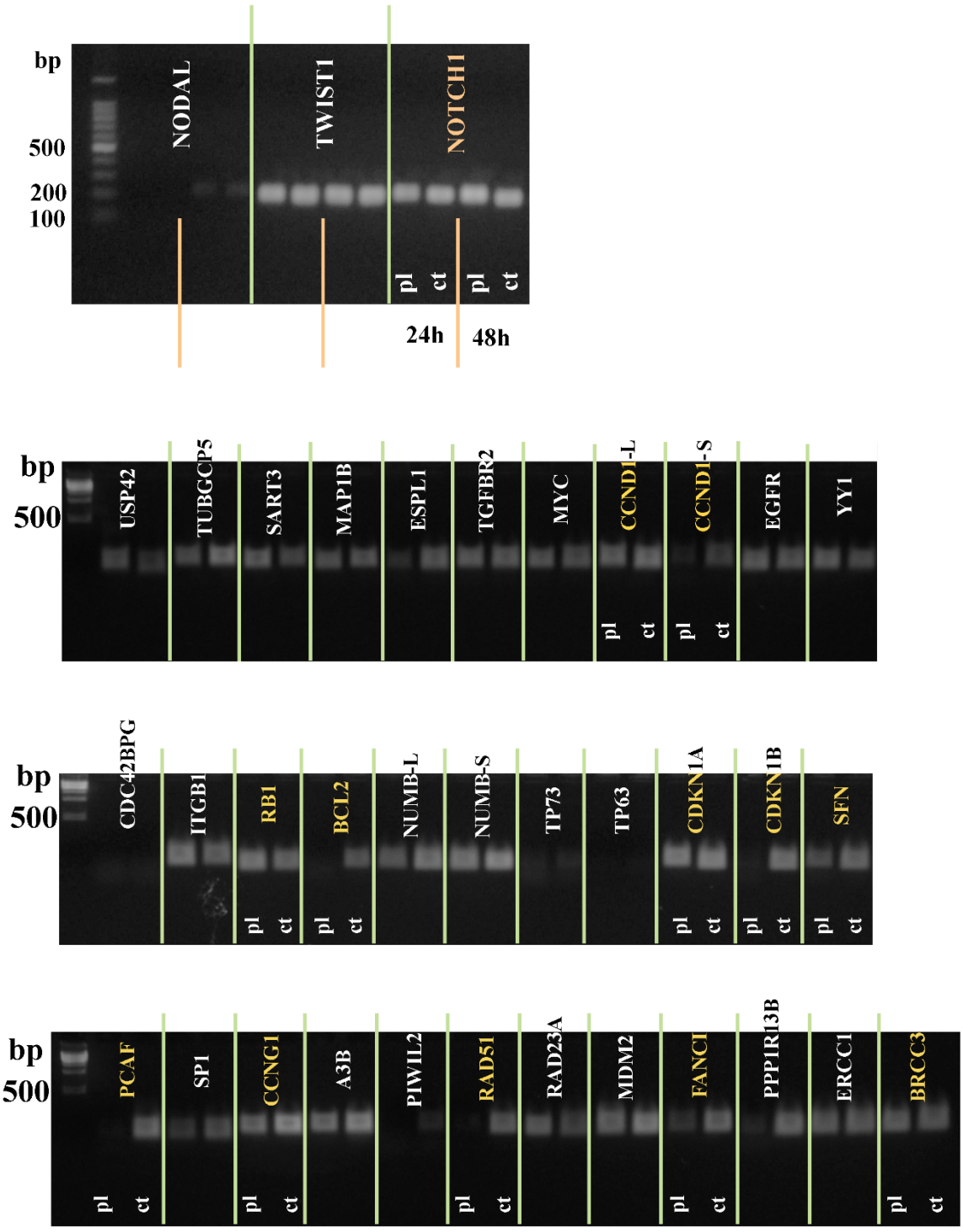

Supplementary Fig. 8. Transcriptional fingerprinting of genes involved in control of cell cycle and intercellular communications. Yellow indicates genes that are utilized in figures of the main manuscript.

Supplementary Data 1. *In-Silico* hybridization of miR4673 to G1 inhibitor gene transcripts demonstrates the lack of proper seeding regions.

CDKN1B

```
mfe: -31.7 kcal/mol

target 5'  G   GG       C   GCCGCAACCAA    U 3'
            CGG  CGGCUCC GCC           UGGA
            GUC  GCCGAGG CGG           ACCU
miRNA  3' AG   AG       A                  5'
```

```
mfe: -30.4 kcal/mol

target 5' C    A G    UUGCCACCCUCUCCG         U 3'
           UCGG C GGCU               CUUGCCUGG
           GGUC G CCGA               GGACGGACC
miRNA  3' A    A G                         U 5'
```

ASPP1

```
mfe: -35.3 kcal/mol

target 5' C     G    AAGCUU      G     G 3'
           CCAGU CCGG      UCCUGU CUGGG
           GGUCA GGCC      AGGACG GACCU
miRNA  3' A          G                  5'
```

KAT2B

```
mfe: -30.8 kcal/mol

target 5' G       C     CU      G 3'
           CUAGUCC  CUCC  CCUGGG
           GGUCAGG  GAGG  GGACCU
miRNA  3' A       CC    AC        5'
```

Supplementary Data 2. Protein homology between human cdk-18 and *Saccharomyces cerevisiae* pho85.

Species	Gene Name	Gene ID	% identity (Protein)	% coverage	Genomic location
Homo sapiens	CDK18	ENSG00000117266	30 %	57 %	1:205504595-205532793
Saccharomyces cerevisiae	Pho85	YPL031C	51 %	94 %	XVI:492018-493037

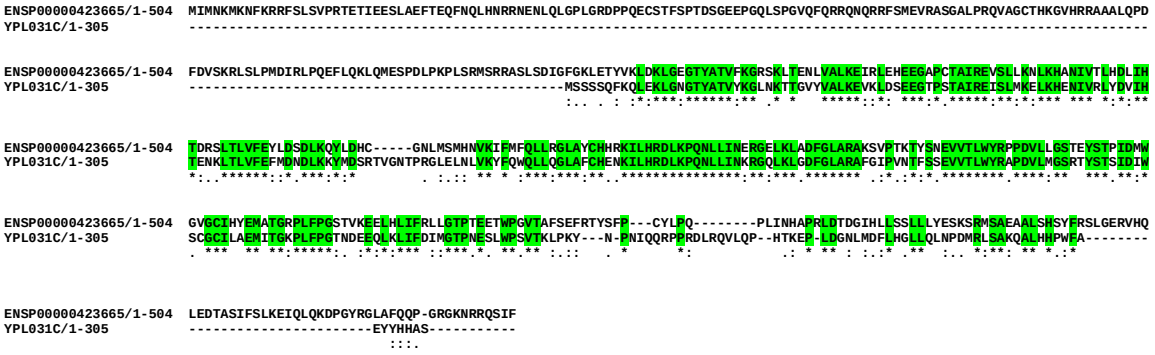

Supplementary tables

Supplementary Table 1. Transcript-specific primers used in the current study.

Gene	Accession No.	Oligos	Primer sequence	Amplicon size (bps)
RAD51	NM_002875.4	F-primer R-primer	TGCCAGCTTCCCATTGACCG CCAGGACATCACTGCCAGAGAG	130
PPP1R13B	NM_015316.2	F-primer R-primer	CCTGCTGGGGCTGTATCCAC AAGTGGCTCCTGGTAGCTGG	101
FANCI	NM_001113378.1	F-primer R-primer	CCCTCCTCTCCTCAGTTTGTGC CGAAACATGCAGGCTGAAGAGCA	123
GADD45A	NM_001924.3	F-primer R-primer	CGTGCTGGTGACGAATCCACA GCCATCACCGTTCAGGGAGAT	148
TP53	NM_000546.5	F-primer R-primer	GCTCAGATAGCGATGGTCTGGC CTCATAGGGCACCACCACACT	131
SFN	NM_006142.3	F-primer R-primer	AGGGTGACTACTACCGCTACCTG GGCATCTCCTTCTTGCTGATGTCC	118
BCL2	NM_000633.2	F-primer R-primer	CTGGTGGACAACATCGCCCTG CAGTTCCACAAAGGCATCCCAGC	99
KAT2B	NM_003884.4	F-primer R-primer	CCTGGAATTAGAGAGACAGGCTGGA GATGGCTCTTCACCTGCTGGA	118
CCNG1	NM_004060.3	F-primer R-primer	GCCTCAGAATGACTGCAAGACTAAGG GGTGCTTGGGCTGTACCTTCA	150
XRCC3	NM_001100119.1	F-primer R-primer	GCATCAACCAGGTGACAGAGGC GGTCAGCCAGCAGTCTCACC	120
BRCA1	NM_007294.3	F-primer R-primer	CAGCTTGACACAGGTTTGGAGTATGC GGCACGGTTTCTGTAGCCCAT	123
BRCA2	NM_000059.3	F-primer R-primer	TTGTGAAGGGTCGTCAGACACC GCACAGTAGAACTAAGGGTGGGTG	117

CUL1	NM_003592.2	F-primer R-primer	TGACAAACTCAGAACCCCTAGACTTGG CGTTCCAACTCTGACGGCAAGG	109
CCND1-short isoform	NM_053056.2 (ENST00000227507.2)	F-primer R-primer	CACCTGGATGCTGGAGATGTGAAG AGGCGGTAGTAGGACAGGAAGTTG	128
CCND1-long isoform	ENST00000536559.1	F-primer R-primer	CTGCTGCAAATGGAGCTGCTC CTGTTTGTTCTCCTCCGCCTCTG	120
CDK18	NM_002596.3	F-primer R-primer	CCGAGAGGTGTCTCTGCTGAAG CAGGTACTCAAACACCAGGGTGAG	103
NOTCH1	NM_017617.4	F-primer R-primer	GCATCTGTGCCAGTACGATGTGG CCGTGTACCCTTCCGTGCA	113
CRB1	NM_201253.2	F-primer R-primer	CGAGGTGGACTTGGCAGATGAC GGAGGTGACAACAGAAGCAACAATGG	115
CDH2	NM_001792.4	F-primer R-primer	GAGCTGACCAGCCTCCAACT TGCATGTGCCCTCAAATGAAACCG	116
CDKN1A	NM_001291549.1	F-primer R-primer	CCTGTCACTGTCTTGTACCCTTGTG GGAGTGGTAGAAATCTGTCATGCTGG	124
CDKN1B	NM_004064.4	F-primer R-primer	CTGAGGACACGCATTTGGTGGA GAGTAGAAGAATCGTCGGTTGCAGG	114
HES1	NM_005524.3	F-primer R-primer	GGATGCTCTGAAGAAAGATAGCTCGC CGGAGGTGCTTCACTGTCATTTCC	81
HEY1	NM_012258.3	F-primer R-primer	CATACGGCAGGAGGGAAAGGTTAC AAGCGGGTCAGAGGCATCTAGT	138
HEY2	XM_017010629.1	F-primer R-primer	GCAACAGGGGGTAAAGGCTACT AGATGAGACACAAGCCGCACC	158
TREK	NM_001017424.2	F-primer R-primer	GGTGACTACGTTGCAGGTGGAT GCAGCAAAGTAAGCAAGCCCTACAA	98
TRPV1	NM_080706.3	F-primer R-primer	TCCAGCAGATGGGCATCTATGC CACCACCGCTGTGGAAAACC	113
RB1	NM_000321.2	F-primer	CCCTTGCATGGCTCTCAGATTCAC	88

		R-primer	GCAGATTCAAGGTGATCAGTTGGTCC	
ACTB	NM_001101.3	F-primer R-primer	AGAGCTACGAGCTGCCTGACG GGACTCCATGCCCAGGAAGGA	101
ATOH1	NM_005172.1	F-primer R-primer	GTGCAGAAGCAGAGACGGCTA GCTCGGACAAGGCGTTGATGTAG	175
MASH1	NM_004316.3	F-primer R-primer	CGGACGAGGGCTCTTACGAC GTGCGATCACCCTGCTTCCA	129
NGN2	NM_024019.3	F-primer R-primer	CGCTGAGGCACAGTTAGAGCC GCTCCTCCTCCTCTTCTTCGTCG	161

Supplementary Table 2. Primers used in stem–loop RT–PCR.

Primer	Utility	Sequence
SL-RT	RT primer	GTCGTATCCAGTGCAGGGTCCGAGGTATTCGCACTGGATACGACGCCGCA
SL-F	Forward primer	CACGCAGTCCAGGCAGGA
SL-R	Reverse primer	CCAGTGCAGGGTCCGAGGTA

Table S3. Primer utilized for detection of endoplasmic reticulum stress.

Gene	Accession No.	Oligos	Primer sequence	Amplicon size (bps)
XBP1-short	NM_001079539.1	F-primer R-primer	CTGAGTCCGAAGCAGGTGCAG ATGCCCAACAGGATATCAGACTCTGA	109
XBP1-long	NM_005080.3	F-primer R-primer	GCAGCACTCAGACTACGTGCA ATGCCCAACAGGATATCAGACTCTGA	127

Supplementary Table 4. Primer used in TRAP assay.

Oligo	Primer sequence
TS (forward)	AATCCGTCGAGCAGAGTT
CX (reverse)	CCCTTACCCTTACCCTTACCCTAA

Supplementary movies

Movie S1. Live-imaging microscopy of mi^{high}Δpl neural progenitors. Note the stationary nature of these G0 synchronised cells.

Movie S2. Type or paste caption here. Live-imaging microscopy of control neural progenitors.

Movie S3. Type or paste caption here. Live-imaging microscopy of mi^{high}Δmi neural progenitors.

Movie S4. Type or paste caption here. Live-imaging microscopy of mi^{low}ΔAs neural progenitors.